# Polymerase Chain Reaction-Free, Sample-to-Answer Bacterial Detection in 30 Minutes with Integrated Cell Lysis

Brian Lam,[†] Zhichao Fang,[‡] Edward H. Sargent,[§] and Shana O. Kelley*[,†,‡,⊥]

[†]Department of Chemistry, Faculty of Arts and Sciences, [‡]Department of Pharmaceutical Sciences, Leslie Dan Faculty of Pharmacy, [§]Department of Electrical and Computer Engineering, Faculty of Engineering, and [⊥]Department of Biochemistry, Faculty of Medicine, University of Toronto, Toronto, Ontario, Canada

ABSTRACT: An important goal for improved diagnosis and management of infectious disease is the development of rapid and accurate technologies for the decentralized detection of bacterial pathogens. Most current clinical methods that identify bacterial strains require time-consuming culture of the sample or procedures involving the polymerase chain reaction.[1−3] Neither of these approaches has enabled testing at the point-of-need because of the requirement for skilled technicians and laboratory facilities. Here, we demonstrate the performance of an effective, integrated platform for the rapid detection of bacteria that combines a universal bacterial lysis approach and a sensitive nanostructured electrochemical biosensor. The lysis is rapid, is effective at releasing intercellular RNA from bacterial samples, and can be performed in a simple, cost-effective device integrated with an analysis chip. The platform was directly challenged with these unpurified lysates in buffer and urine. We successfully detected the presence of bacteria with high sensitivity and specificity and achieved a sample-to-answer turnaround time of 30 min. We have met the clinically relevant detection limit of 1 cfu/μL, indicating that uncultured samples can be analyzed. This advance will greatly reduce time to successful detection from days to minutes.
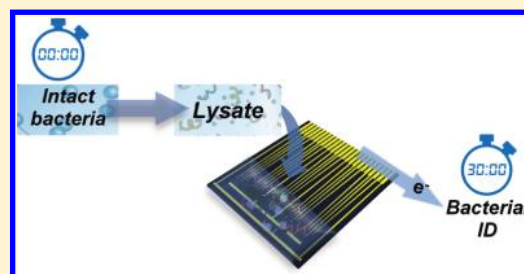
The effective management of infectious disease caused by bacterial pathogens is a major problem in clinical medicine that is hampered by the lack of rapid diagnostic methods.[1−4] Approaches currently used for correct diagnosis of infectious bacterial strains include phenotypic testing and assays that rely on the polymerase chain reaction (PCR).[3,5,6] Many methods require a time-consuming culture step that takes days to weeks depending on the strain of bacteria, and phenotypic testing to confirm antibiotic resistance can double the diagnosis time. To speed analysis, PCR may also be performed on cultured samples or in some cases uncultured samples; however, this approach typically requires stringent purification of nucleic acids. The delays in the availability of diagnostic information limits the effectiveness of treatment. Hence, there is need for a rapid platform that can classify bacterial species.

A great deal of effort has gone into the development of point-of-need methods to meet the challenge of rapid bacterial identification;[7−10] most of the methods developed rely on PCR and face inherent limitations because of the requirement for enzymatic components and thermal control. In addition, methods based on surface plasmon resonance,[11−13] quartz crystal microbalance,[14,15] and fluorescence[16,17] have been reported with good detection limits. However, many of these are immunological[11,12,14,16] and are ineffective at providing genetic-level information required for strain typing. Furthermore, these methods can require labeled markers[13,15] and additional optical[11−13,16,17] and/or fluid handling systems,[7−10,12,13,15] which adds to their complexity, cost, and lack of applicability to point-of-care testing.

Work in our laboratories has focused on developing an electrochemical strategy that combines ultrasensitive detection, straightforward sample processing, and inexpensive components that can be integrated into a cost-effective, user-friendly device. Our detection platform combines an electrochemical reporter system and nanostructured microelectrodes (NMEs) (Figure 1A,B) to detect specific nucleic acid sequences that hybridize to probe molecules immobilized on the sensors. We have previously shown that the NME platform is highly sensitive, with a tunable degree of sensitivity,[18,19] and highly selective.[20,21] Moreover, it is multiplexed and scalable, with straightforward photolithography used for fabrication that is highly versatile.

While prior efforts to exploit this platform for RNA detection showed that very high levels of performance could be achieved both with bacterial and mammalian targets,[22,23] integrated sample processing, an essential feature for a point-of-care diagnostic device, had not yet been addressed. We therefore explored a processing approach that would be complementary to our electronic readout strategy: electrical cell lysis. Alternative methods that could be used for this purpose include chemical, physical,[24,25] and thermal lysis methods.[26] However, the addition of chemical agents, complicated device geometries, or thermal elements are undesirable given that they can introduce interfering agents or increase the complexity of the device. Electrical lysis of bacterial cells has been well studied
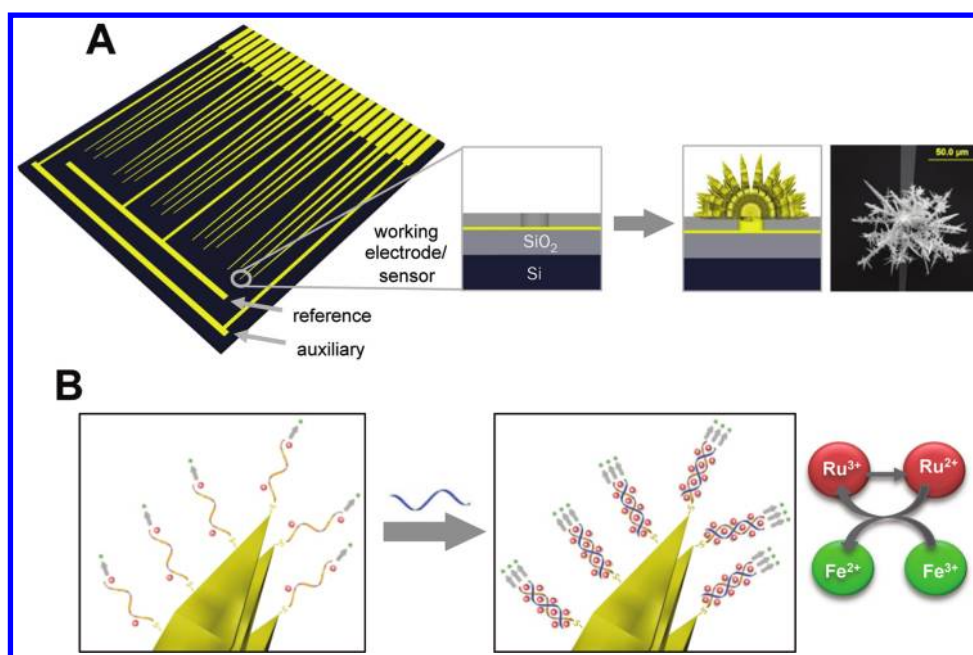
Figure 1. Bacterial detection sensors. (A) The NME platform consisting of Si chip with patterned Au working, reference, and auxiliary electrodes. The working electrode surface is passivated with SiO_2, and 5 μm apertures are etched at the tip of each electrode. NMEs are electroplated within each aperture, with a typical size of ~100 μm. (B) Electrochemical detection scheme for nucleic acids utilizing Ru^{3+} and Fe^{3+} electrocatalytic reporter pair.

in the past.[27−30] The major drawback is that high electric field requirements, greater than 10 kV/cm, are required to lyse bacterial cells, which has limited its use for inline sensing. Prior work in our laboratories utilized microfludic lysis chambers[31,32] which take advantage of geometrical field effects to lower applied voltages. However, voltage requirements were still high (1000 V). In addition, this and other systems[33] require fluidics that can only analyze small sample volumes and increase processing times.

To address these issues, we hypothesized that, by assembling a chamber composed of two conductive gold electrodes with a very thin spacer (~500 μm), we could lyse bacteria introduced to the electrodes with an applied potential. If this type of sample processing module was coupled with a NME chip (Figure 2A), it could be used to achieve rapid sample-to-answer bacterial detection with minimal intervention by the user (Figure 2B). The workflow used here involved: (1) a solution being introduced into the chamber with a syringe, (2) lysis being induced with an applied field, (3) the sample being moved to the chip with an injection of air, (4) mixing with reporter groups, and (5) readout. This workflow can be completed in less than 30 min and permits bacterial identification and classification.

■ METHODS

Chip Fabrication. Detection chips were fabricated using 6 in. thin silicon wafers passivated with a thick thermally grown silicon oxide layer. First, a positive photoresist was patterned to the desired electrical contact and lead structure using standard photolithographic methods. Subsequently, a 500 nm gold layer was deposited using electron-beam assisted gold evaporation, and a standard lift off process was used to expose the desired contact and lead structure. Next, a second layer of 500 nm silicon dioxide was deposited to passivate the lead structure using chemical vapor deposition. Finally, 5 μm apertures were

etched into the second passivating silicon dioxide layer, exposing the gold layer at the end of each lead structure.

Nanostructured Microelectrode (NME) Fabrication. Chips were cleaned by sonicating in acetone for 1 min and rinsing with isopropanol and deionized water for 30 s. NMEs were electroplated using a standard 3 electrode system featuring a Ag/AgCl reference, platinum auxiliary electrode and the 5 μm gold aperture as the working electrode. An electroplating solution of 20 mM $HAuCl_4$ in 0.5 M HCl was used. The substructures of NMEs were plated by holding each electrode at 0 mV for 250 s. Finally, a nanostructured overlayer was plated by holding the electrode at −700 mV for 10 s.

Synthesis and Purification of Peptide Nucleic Acid Probes. PNA probes were synthesized in house using a Protein Technologies Prelude peptide synthesizer. The following probe sequences specific to the rpoβ mRNA were utilized for detection of unpurified lysates: NH$_2$-*Cys-Gly-Asp*-ATC TGC TCT GTG GTG TAG TT-*Asp*-CONH$_2$ (*E. coli*) and NH$_2$-*Cys-Gly-Asp*-AAG TAA GAC ATT GAT GCA AT-*Asp*-CONH$_2$ (*S. saprophyticus*). All probes were stringently purified by reverse phase high performance liquid chromatography. Probe sequences were quantified by measuring absorbance at 260 nm, and excitation coefficients were obtained from http://www.panagene.com

Modification of NMEs with PNA probes. A solution of 1 μM purified thiolated PNA probe in 25 mM NaCl was deposited onto the surface of an NME chip in a dark humidity chamber overnight at room temperature. A dam constructed from adhesive silicone spacers was used to deposit two different probes on each NME chip.

Bacterial Samples. *Escherichia coli* was obtained from Invitrogen (18265-017). *Staphylococcus saprophyticus*, methicillin-resistant *Staphylococcus aureus*, and methicillin-susceptible *Staphylococcus aureus* was obtained from ATCC (ATCC 15305, BAA-1720, 29213). All strains were grown in the appropriate growth media in an incubating shaker at 37 °C. After growth to
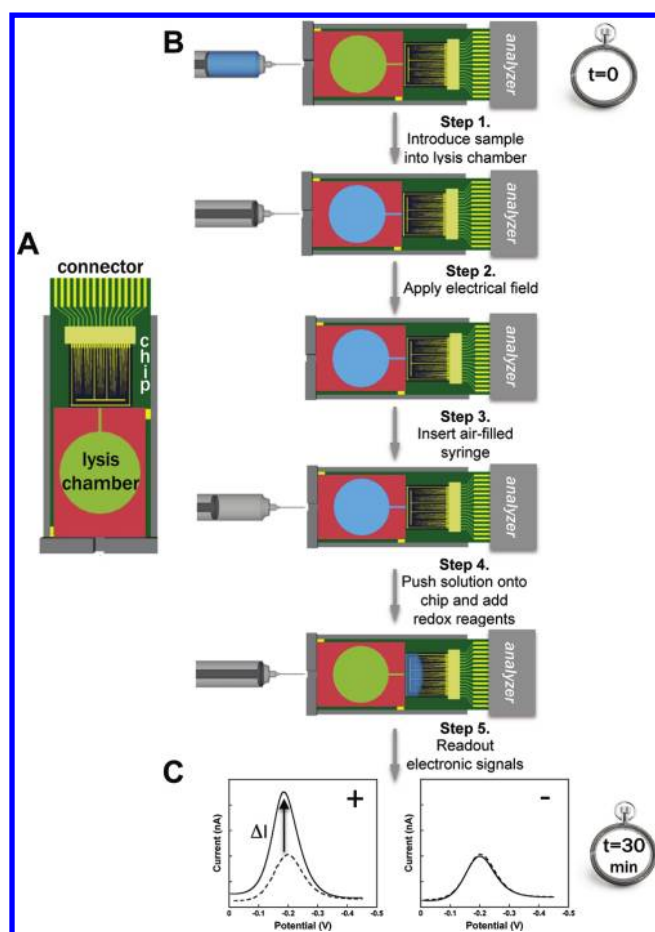
Figure 2. Integrated sensing system. (A) Schematic of cartridge integrating lysis chamber, NME chip, and connector to analyzer. (B) Overview of detection scheme; injection, lysis, delivery, and readout in 30 min. (C) Typical differential pulse voltammograms of positive (left) and negative (right) samples where the dotted line is the background and the solid line is the readout.

the desired population, the growth media was replaced with 1× PBS.

Lysis Chamber Fabrication and Operation. Lysis chambers were fabricated using adhesive silicone hybridization spacers (0.5 × 25 × 25 mm) obtained from Grace Biolabs and gold coated slides (25 × 25 mm) obtained from EMF Corporation. Chambers were constructed by first cutting a narrow channel ~1 mm wide into the spacer, which was then sandwiched between two gold slides. To lyse the bacterial samples, a 200 μL suspension was loaded into the chamber using a syringe and 100 V, 10 ms DC pulses were applied to the sample at a frequency of 1 Hz for 20 s.

Hybridization Protocol and Electrochemical Measurements. Electrochemical measurements were made using a PalmSens EmStat embedded potentiostat. After modification of NMEs with PNA probes, a background signal was scanned in electrocatalyic buffer containing 10 μM Ru(NH$_3$)$_6^{3+}$ and 1 mM Fe(CN)$_6^{3-}$ in 0.1× PBS. Immediately after lysis, NMEs were incubated with unpurified lysates for 20 min at 37 °C. After hybridization, chips were washed twice in 0.1× PBS. We subsequently scanned the hybridization signal after incubation in the same electrocatalytic buffer.

Reverse-Transcriptase Polymerase Chain Reaction. Primer sequences specific to a 185 bp region of the *E. coli* rpoβ

mRNA were synthesized. A Qiagen one-step RT-PCR kit (210210) was used to perform RT-PCR on lysates. After lysis, samples were centrifuged at 10 000 rpm to remove intact bacterial cells that would generate a positive signal. RT-PCR was then performed on the supernatant. The products were visualized using agarose gel electrophoresis and ethidium bromide fluorescent stain.

Flow Cytometry. Flow cytometry measurements were made utilizing a BD FACS Canto Instrument. After lysis, samples were incubated in propidium iodide in the dark at room temperature at a concentration of 25 μg/mL for 30 min before injection into the flow cytometer. Counts versus fluorescence intensity measurements were made in the red channel of the flow cytometer.

■ RESULTS AND DISCUSSION

To validate our lysis approach, we examined samples of two model organisms, *Escherichia coli* (EC) and *Staphylococcus saprophyticus* (SS). Bacterial samples suspended in buffered solution were introduced into the lysis chamber and lysed with varying voltages (0−100 V) and pulse widths (0−10 ms). A small amount of bubbling was observed, but the escape of these bubbles could be controlled by minimizing the width of the exit port on the lysis chamber. To assess lysis efficiency, we first looked at cell viability after lysis by monitoring growth on agar plates. With applied voltages as low as 2 V, all of the bacteria in processed samples were killed (data not shown). This loss in viability, however, cannot be used as an unequivocal test for cell lysis, as it does not indicate whether the bacterial cell walls were compromised prior to cell death. Therefore, to confirm that the applied electrical fields did cause irreversible cell rupture, we analyzed propidium iodide (PI) uptake using flow cytometry. PI fluoresces only when intercalated with DNA and does not cross uncompromised cell walls and, therefore, can be used as an indicator of cell lysis. After incubation in PI, samples were analyzed using flow cytometry and histograms of counts versus fluorescence intensity were plotted versus different pulse widths (Figure 3A) and applied voltages (Figure 3B).

Interestingly, when the lysis of SS was monitored, it was observed that larger voltages were required to trigger PI uptake relative to those needed to cause cell death as observed on a culture plate. This indicates that cellular death alone is not proof of cellular lysis. Another interesting observation that emerged from these studies was that lower voltages caused PI uptake in EC relative to SS, indicating that voltages must be tailored for gram-negative bacteria versus gram-positive bacteria and that tailored pulse structures could potentially be used for selective lysis. We also explored the feasibility of lysing *Staphylococcus aureus* (SA) and methicillin-resistant SA and observed successful cell rupture for these organisms (Figure 3C). These results verify that the approach is generally applicable to bacterial organisms.

To confirm that the PI uptake monitored in the experiments described above corresponded to the release of nucleic acids, we used the reverse-transcriptase polymerase chain reaction (RT-PCR) to confirm the release of intercellular RNA targets from EC. Shown in Figure 3D are RT-PCR measurements that were performed on the supernatant of lysed and unlysed samples in Figure 3B. A positive control lysed with isopropanol was used for the calculation of relative PCR efficiency. The 180 bp RT-PCR products were visualized on an agarose gel where the correct primer specific products were verified. The intensity of the product bands observed was directly proportional to the
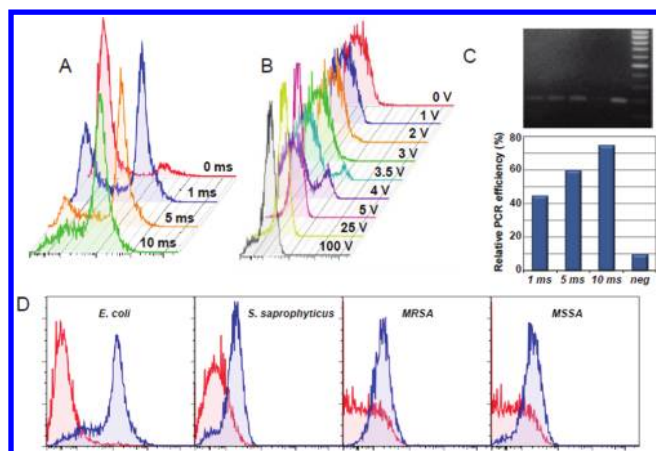
Figure 3. Characterization of electrically lysed bacterial solutions. (A) Flow cytometry histograms of propidium iodide uptake versus pulse width (100 V, 1 Hz, 20 s) collected with *E. coli*. Increasing the pulse duration decreases the number of unlysed cells. (B) Flow cytometry measurements of *S. saprophyticus* lysed at different voltages (10 ms, 1 Hz, 20 s) showing effective lysis down to 5 V. (C) RT-PCR measurements on *E. coli*. The PCR targeted a 185 bp region within the *rpoB* mRNA. Pulse durations were 1 ms, 5 ms, and 10 ms. A negative (no applied potential) and positive control (isopropanol-based lysis) were also run. Relative PCR efficiency was established by comparison with a postive control sample that was lysed with isopropanol (lane next to DNA ladder). (D) Flow cytometry measurements from lysis of *E. coli*, *S. saprophyticus*, MRSA, and MSSA. The red trace represents the unlysed control, and blue is the lysed sample (100 V, 10 ms, 1 Hz, 20 s).

pulse width and correlated well with the amount of PI uptake observed.

To validate that this sample processing approach could be used with our NME detection platform, we directly challenged our sensors with unpurified lysates generated using our lysis chamber. Our NME detectors are fabricated on the surface of silicon wafers using traditional photolithographic methods[19] (Figure 1A). This NME sensor chip includes 20 working electrodes and on-board auxiliary and reference electrodes. Gold NMEs are electroplated into 5 μm apertures at the surface of each working electrode using a gold salt plating solution. The size and morphology of structures can be controlled through varying applied voltage and plating solution as previously described.[19] NME structures used for this study were ~100 μm in diameter.

Detection of nucleic acids was achieved using an electrocatalytic method developed in our laboratory.[34,35] The method is depicted in Figure 1B, where the bare NMEs are first functionalized with target specific peptide nucleic acid (PNA) probe molecule. PNA probes, possessing a neutral backbone, bind to complementary strands with higher affinity and selectivity than their DNA analogues.[36] The electrocatalytic reporter pair consists of $Ru(NH_3)_6^{3+}$ and $Fe(CN)_6^{3-}$. $Ru(NH_3)_6^{3+}$ is electrostatically attracted to anionic nucleic acids that accumulate on the surface of the NME. $Ru(NH_3)_6^{3+}$ is therefore accumulated at the NME surface if the complementary nucleic acid target is bound to the PNA probe. Using differential pulse voltammetry (DPV), the surface of the NME is scanned over a specified potential window before and after hybridization. Reduction of $Ru(NH_3)_6^{3+}$ to $Ru(NH_3)_6^{2+}$ occurs near the surface when the Ru(III) reduction potential is reached. $Fe(CN)_6^{3-}$ then oxidizes $Ru(NH_3)_6^{2+}$ back to

$Ru(NH_3)_6^{3+}$, generating an electrocatalytic current. Typical positive and negative DPV are shown in Figure 2D.

The use of this method with unpurified lysates of EC and SS generated using electrical lysis is demonstrated in Figure 4A,B.
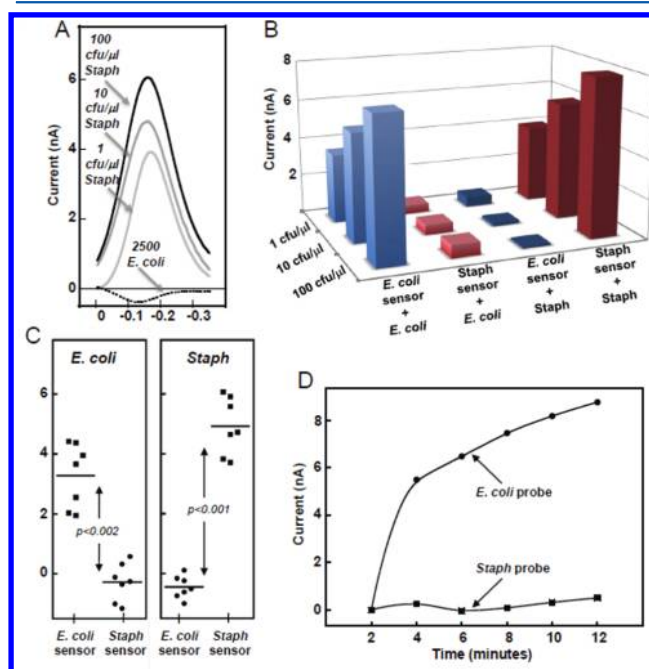

Figure 4. Direct bacterial detection in unpurified lysates (A) Representative background-subtracted electrochemical differential pulse voltammograms used for study of sensitivity and specificity. The data shown was collected with the SS probe directly challenged with the corresponding unpurified lysates. (B) Background-subtracted peak currents of sensors challenged with unpurified lysates demonstrating sensitivity and specificity. Values shown represent averages of >6 trials; coefficient of variation was <20%. (C) Direct detection of *E. coli* and *S. saprophyticus* in urine samples. Sensors were challenged directly with unpurified lysates of spiked urine samples for 30 min prior to electrochemical analysis. A control probe was used in each trial to assess background signals. A current value was collected for each trial and was plotted individually. (D) Real-time analysis of a 100 cfu/uL *E.coli* lysate spiked with the electrocatalytic reporter groups. A differential pulse voltammogram was measured at each time point for both complementary and noncomplementary sensors, and peak currents were plotted as a function of time.

NME sensors were modified with probes corresponding to the sequence of the RNA polymerase β mRNA found in EC or SS. The lysed bacteria were introduced, and electrochemical signals were obtained within 30 min. Typical background subtracted DPV measurements obtained at NME sensors are shown in Figure 4C. Evaluation of limits of detection (Figure 4B) verify that this approach is successful with as few as 1 bacterial cell per microliter, a concentration that corresponds to the levels of bacteria found in many types of clinical samples. A limited dynamic range was explored in this study, but if analysis of a larger range of concentrations was desired, prior work on the use of sensor nanostructuring[19] and size[20] could be leveraged to widen dynamic range.

To validate applicability of our integrated platform to samples resembling those relevant for clinical analysis, we challenged it with samples of urine spiked with both EC and SS. This analysis simulates real-world urinary tract infections where the relevant threshold is ~100 cfu/μL.[37] After crude urine

samples were lysed, they were directly applied to NME sensors specific to EC and SS. Successful detection of both EC and SS was achieved even in the presence of this complex biological background (Figure 4C).

The adaptation of this approach to real-time detection was investigated, with signals being collected during hybridization of NME sensors with an unpurified lysate. This analysis was done in "one-pot", with reporter groups present during hybridization. Specific detection of EC could be achieved using this approach, with very rapid readout achieved within minutes at a concentration of this pathogen that corresponds to its levels in samples collected from patients with a urinary tract infection (Figure 4D). This indicates that a positive result could be obtained from this type of sample within 2 min, a significant improvement over the culture-based methods typically employed for this type of analysis.

■ CONCLUSIONS

The advances reported here demonstrate the first PCR-free, chip-based sensing system to provide sample-to-answer sensing of bacterial pathogens at clinically relevant levels. A simple lysis chamber was used to trigger electrical rupture of bacteria, and these crude lysates, generated in buffer or urine, were directly analyzed with an ultrasensitive microchip featuring nano-structured microsensors. Real-time analysis is also enabled by the robust sensors that are resistant to fouling by cellular contents.

■ AUTHOR INFORMATION

Corresponding Author
*E-mail: shana.kelley@utoronto.ca.

■ ACKNOWLEDGMENTS

■ REFERENCES

(1) Greenwood, D. *J. Infect. Dis.* **1981**, *144*, 380−385.

(2) Rantakokko-Jalava, K.; Jalava, J. *J. Clin. Microbiol.* **2002**, *40*, 4211−4217.

(3) Tang, Y. W.; Stratton, C. W. *Advanced techniques in diagnostic microbiology*; Springer: New York; 2006.

(4) Levy, S. B.; Marshall, B. *Nat. Med.* **2004**, *10*, S122−S129.

(5) Clinical and Laboratories Standards Institute. *CLSI document M02-A10*; Clinical and Laboratories Standards Institute: Pennsylvania, 2009.

(6) Clinical and Laboratories Standards Institute. *CLSI document M100-S21*; Clinical and Laboratories Standards Institute: Pennsylvania, 2011.

(7) House, D. L.; Chon, C. H.; Creech, C. B.; Skaar, E. P.; Li, D. Q. *J. Biotechnol.* **2010**, *146*, 93−99.

(8) Liu, R. H.; Yang, J. N.; Lenigk, R.; Bonanno, J.; Grodzinski, P. *Anal. Chem.* **2004**, *76*, 1824−1831.

(9) Shen, F.; Du, W.; Kreutz, J. E.; Fok, A.; Ismagilov, R. F. *Lab Chip* **2010**, *10*, 2666−2672.

(10) Yeung, S. W.; Lee, T. M. H.; Cai, H.; Hsing, I. M. *Nucleic Acids Res.* **2006**, *34*, 7.

(11) Oh, B. K.; Kim, Y. K.; Park, K. W.; Lee, W. H.; Choi, J. W. *Biosens. Bioelectron.* **2004**, *19*, 1497−1504.

(12) Subramanian, A.; Irudayaraj, J.; Ryan, T. *Biosens. Bioelectron.* **2006**, *21*, 998−1006.

(13) He, L.; Musick, M. D.; Nicewarner, S. R.; Salinas, F. G.; Benkovic, S. J.; Natan, M. J.; Keating, C. D. *J. Am. Chem. Soc.* **2000**, *122*, 9071−9077.

(14) Su, X. L.; Li, Y. B. *Biosens. Bioelectron.* **2004**, *19*, 563−574.

(15) Mao, X. L.; Yang, L. J.; Su, X. L.; Li, Y. B. *Biosens. Bioelectron.* **2006**, *21*, 1178−1185.

(16) Ko, S. H.; Grant, S. A. *Biosens. Bioelectron.* **2006**, *21*, 1283−1290.

(17) Edgar, R.; McKinstry, M.; Hwang, J.; Oppenheim, A. B.; Fekete, R. A.; Giulian, G.; Merril, C.; Nagashima, K.; Adhya, S. *Proc. Natl. Acad. Sci. U.S.A.* **2006**, *103*, 4841−4845.

(18) Bin, X. M.; Sargent, E. H.; Kelley, S. O. *Anal. Chem.* **2010**, *82*, 5928−5931.

(19) Soleymani, L.; Fang, Z. C.; Sargent, E. H.; Kelley, S. O. *Nat. Nanotechnol.* **2009**, *4*, 844−848.

(20) Fang, Z.; Soleymani, L.; Pampalakis, G.; Yoshimoto, M.; Squire, J. A.; Sargent, E. H.; Kelley, S. O. *ACS Nano* **2009**, *3*, 3207−3213.

(21) Yang, H.; Hui, A.; Pampalakis, G.; Soleymani, L.; Liu, F.-F.; Sargent, E. H.; Kelley, S. O. *Angew. Chem., Int. Ed.* **2009**, *48*, 8461−8464.

(22) Soleymani, L.; Fang, Z.; Lam, B.; Xiaomin Bin, X.; Vasilyeva, E.; Ross, A. J.; Sargent, E. H.; Kelley, S. O. *ACS Nano* **2011**, *5*, 3360−3366.

(23) Vasilyeva, E.; Lam, B.; Fang, Z.; Minden, M. D.; Sargent, E. H.; Kelley, S. O. *Angew. Chem.* **2011**, *123*, 4223−4227.

(24) Huh, Y. S.; Choi, J. H.; Park, T. J.; Hong, Y. K.; Hong, W. H.; Lee, S. Y. *Electrophoresis* **2007**, *28*, 4748−4757.

(25) Di Carlo, D.; Jeong, K. H.; Lee, L. P. *Lab Chip* **2003**, *3*, 287−291.

(26) Privorotskaya, N.; Liu, Y.-S.; Lee, J.; Zeng, H.; Carlisle, J. A.; Radadia, A.; Millet, L.; Bashir, R.; King, W. P. *Lab Chip* **2010**, *10*, 1135−1141.

(27) Grahl, T.; Markl, H. *Appl. Microbiol. Biotechnol.* **1996**, *45*, 148−157.

(28) Hulsheger, H.; Potel, J.; Niemann, E. G. *Rad. Environ. Biophys.* **1983**, *22*, 149−162.

(29) Sale, A. J. H.; Hamilton, W. A. *Biochim. Biophys. Acta* **1967**, *148*, 781−788.

(30) Hamilton, W. A.; Sale, A. J. H. *Biochim. Biophys. Acta* **1967**, *148*, 789−800.

(31) Wang, H. Y.; Bhunia, A. K.; Lu, C. *Biosens. Bioelectron.* **2006**, *22*, 582−588.

(32) Bao, N.; Lu, C. *Appl. Phys. Lett.* **2008**, *92*, 3.

(33) Lee, S. W.; Tai, Y. C. *Sens. Actuators, A* **1999**, *73*, 74−79.

(34) Gasparac, R.; Taft, B. J.; Lapierre-Devlin, M. A.; Lazareck, A. D.; Xu, J. M.; Kelley, S. O. *J. Am. Chem. Soc.* **2004**, *126*, 12270−12271.

(35) Lapierre, M. A.; O'Keefe, M.; Taft, B. J.; Kelley, S. O. *Anal. Chem.* **2003**, *75*, 6327−6333.

(36) Nielsen, P. E. *Acc. Chem. Res.* **1999**, *32*, 624−630.

(37) Aguirre-Avalos, G.; Zavala-Silva, M. L.; Díaz-Nava, A.; Amaya-Tapia, G.; Aguilar-Benavides, S. *Arch. Med. Res.* **1999**, *30*, 29−32.